EUROPHYSICS LETTERS 1 June 2001

Europhys. Lett., **54** (5), pp. 675–681 (2001)

Correlation of tunneling spectra with surface nanomorphology and doping in thin $YBa_2Cu_3O_{7-\delta}$ films

A. Sharoni[1], G. Koren[2] and O. Millo[1](*)

[1] *Racah Institute of Physics, The Hebrew University - Jerusalem 91904, Israel*

[2] *Department of Physics, Technion-Israel Institute of Technology, Haifa 32000, Israel*

(received 25 January 2001; accepted in final form 29 March 2001)

PACS. 74.50.+r – Proximity effects, weak links, tunneling phenomena, and Josephson effects.
PACS. 74.72.Bk – Y-based cuprates.
PACS. 74.80.-g – Spatially inhomogeneous structures.

Abstract. – Tunneling spectra measured on thin epitaxial $YBa_2Cu_3O_{7-\delta}$ films are found to exhibit strong spatial variations, showing U- and V-shaped gaps as well as zero-bias conductance peaks typical of a d-wave superconductor. A full correspondence is found between the tunneling spectra and the surface morphology down to a level of a unit-cell step. Splitting of the zero-bias conductance peak is seen in optimally doped and overdoped films, but not in the underdoped ones, suggesting that there is no transition to a state of broken time-reversal symmetry in the underdoped regime.

The d-wave nature of superconductivity in $YBa_2Cu_3O_{7-\delta}$ (YBCO) and some other high-T_c superconductors is well established by now [1, 2]. In particular, various groups have reported directional tunneling and point contact spectroscopy measurements that exhibit a dominant $d_{x^2-y^2}$ symmetry for the order parameter of YBCO [3–8]. However, the spatial variation of the electronic properties in the superconducting state and its correlation with the surface morphology has not been reported for this system. These properties are reflected in the quasi-particle density of states (DOS), which can be measured by tunneling spectroscopy [9]. Such studies are important for resolving various open problems regarding the nature of superconductivity in YBCO. For example, contrary to theoretical predictions [10, 11], zero-bias conductance peaks (ZBCP) due to surface Andreev bound state (ABS) were commonly observed when tunneling was nominally in the [100] direction [3–5]. This was attributed, but not yet demonstrated experimentally, to faceting and microscopic roughness that reveal the (110) face at which ABS are expected to reside [3, 5, 12]. Another intriguing issue is that of the emergence of a state with broken time-reversal symmetry at the surface due to the existence of a subdominant order parameter with $\pi/2$ phase difference relative to the dominant $d_{x^2-y^2}$ symmetry [12, 13]. This phenomenon manifests itself as a splitting of the ZBCP in zero magnetic field at low enough temperatures. Such a splitting was observed by

(*) E-mail: milode@vms.huji.ac.il

© EDP Sciences

some groups [4,5] but not by others [6,8,14] and it was shown by Deutscher that the splitting might depend on the doping level [5, 15]. Therefore, since the doping level may fluctuate spatially over the surface even on a submicrometer scale [16, 17], the nature of the ZBCP and its splitting should consequently exhibit strong spatial variations. In the present study we exploit the high spatial resolution enabled by scanning tunneling microscopy (STM) and spectroscopy for the investigation of the above issues.

Extensive STM studies of high-T_c superconductors have been performed in recent years [18]. These include atomically resolved investigations of the role of disorder in YBCO [19], as well as the effects of atomic-size impurities on the local quasi-particle DOS in a single crystal of $BiSr_2CaCu_2O_8$ (BSSCO) that portray the d-wave nature of this superconductor [20, 21]. However, the effect of larger-scale topographic features, such as microfacets and unit-cell steps, on the local DOS was not yet treated, and this is the main focus of our present STM study of ultrathin YBCO films. Our tunneling spectra exhibit pronounced spatial variations that are well correlated with the surface morphology. We show that a single unit-cell step on the *ab*-surface is sufficient to induce a ZBCP when tunneling along the *c*-axis. Moreover, splitting of the ZBCP was found in various locations (but not everywhere) on nominally (as prepared) overdoped and optimally doped samples, but was never observed in the underdoped films, consistently with ref. [15].

Epitaxial YBCO films of 200–300 Å thickness were grown on (100) $SrTiO_3$ wafers by laser ablation deposition, with *c*-axis orientation normal to the substrate. Films of different doping levels were obtained by the use of different annealing conditions immediately after the deposition process. Annealing at 0.8 atm oxygen pressure with a dwell of 1 h at 450 C yielded optimally or slightly overdoped films with $T_c \sim 90$ K, while a cool-down under 20 mTorr oxygen flow at 900 C/h yielded an underdoped phase of $T_c \sim 60$–70 K. The T_c of our films was uniform up to about 0.5 K, as measured at 10 different points over the 1 cm^2 area of the wafer. X-ray diffraction analysis and the structure of the $R(T)$ curves (not shown here) confirmed the doping levels of these phases. At a relatively low deposition rate and small laser power, the films consisted of crystallites having well-defined facets, as depicted in fig. 1a. The crystallite structure became less clear upon increasing of the laser power, and the dominant surface structures revealed by the STM images were voids and island of one unit-cell height (fig. 2a). The rich surface morphology of these films enabled the observation of a wealth of spectral structures and the study of their spatial dependence, as shown below. The films were taken out from the growth chamber and transferred in a dry atmosphere to a cryogenic STM within a few hours. The onset of the superconducting transition did not change during this transfer process, but the transition width increased considerably from about 1 K for freshly prepared films to around 10 K after completing the STM measurements. The tunneling spectra (dI/dV *vs.* V characteristics) were acquired either directly by the use of conventional lock-in technique, or by numerical differentiation of the measured I-V curves, with similar results obtained by both methods. We have checked the dependence of the tunneling spectra on the voltage and current setting (*i.e.*, the tip-sample distance) and found it not to affect the measured gap and ZBCP features. However, the setting did influence the background, in particular the degree of asymmetry the spectra exhibit, as noted previously by various groups [22].

A typical correlation between the tunneling spectra and the local surface morphology is depicted in fig. 1, measured on an optimally doped film, which focuses on a nearly square-shaped crystallite about 50 nm long and 17 nm high (fig. 1a). On top of this crystallite, V-shaped gap structures were observed, as shown by the curve acquired at position labelled 1 in this image, presented in fig. 1b (solid line). In general, spectra measured on such positions showed fluctuations in the degree of asymmetry, in the sharpness of the gap-edge shoulders

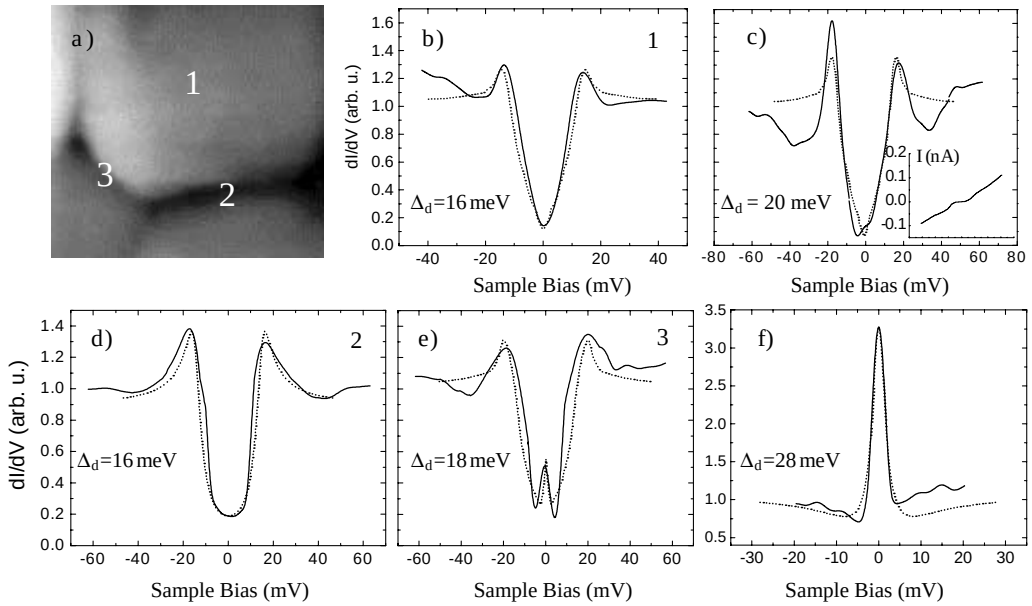

Fig. 1 – Correlation between tunneling spectra (at 4.2 K) and the surface morphology of a thin YBCO film. a) 50×50 nm^2 STM topographic image showing four crystallites and the interfaces between them. The numbers 1-3 denote the positions where spectra b, d and f were acquired. b)-f) Tunneling spectra measured at different locations (black lines), where b)-e) were taken on the same sample and f) on a different one. The dotted curves are fits to the theory of tunneling into a d-wave superconductor with order parameters, Δ_d, denoted in the figures. The spectra exhibit various structures that manifest d-wave superconductivity: b) V-shaped gap for the curve measured on top of a crystallite (position 1), typical for c-axis tunneling. c) Asymmetric V-shaped gap with a small zero-bias structure (measured on top of another crystallite); the I-V curve is presented in the inset. d) U-shaped gap for the spectrum taken at the interface position 2, where the (100) face is revealed. e) ZBCP inside a gap structure for the curve measured near a corner position 3, showing contributions of (100), (110) and (001) faces. f) A pure ZBCP structure taken on a (110) facet.

and in the possible existence of small zero-bias anomalies (see below), but not in the general V-shaped structure as expected for tunneling in the c-direction. This is due to the finite tunneling-cone width in the STM experiment that allows coupling to the electronic states in the CuO_2 planes. The general structure of this dI/dV-V curve is well reproduced by a simulation based on the formalism for tunneling into a d-wave superconductor [10, 11], assuming tunneling in the c-direction (dotted curve). In many cases a small structure (far from being a well-developed ZBCP) appears at around zero bias, as exhibited by the curve in fig. 1c, taken on top of a different crystallite. Similar structures were found by other groups on c-axis BSSCO crystals and attributed to impurity-induced quasi-particle excitation at the Fermi level [20, 21, 23, 24]. Enhanced gap-edge shoulders, as seen in the spectrum, have also been observed previously [3,14,21] and were related to a van-Hove singularity in the electronic DOS [14].

The tunneling spectra obtained when positioning the tip above a crystallite edge look considerably different when either the (100) or the (110) planes are probed. A nearly U-shaped gap structure is obtained at position 2 (fig. 1d), as well as in any other position along the same facet, suggesting that the (100) face is exposed at this edge, as confirmed by

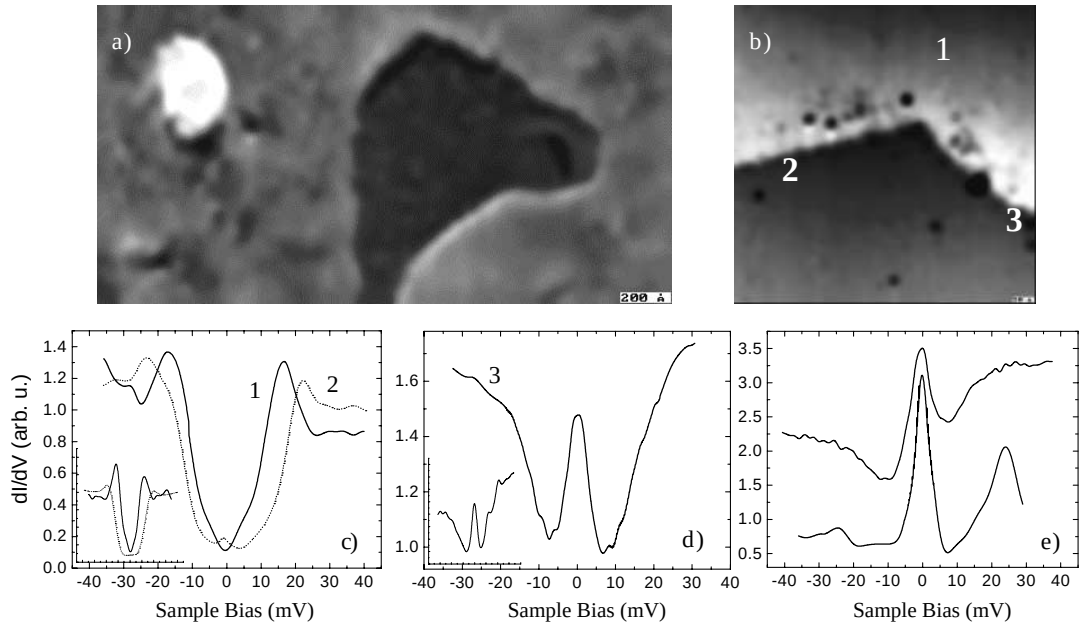

Fig. 2 – The effect of steps of unit-cell height on the tunneling spectra measured on a slightly overdoped film. a) and b) Topographic images of size 120×220 and 120×120 nm^2, respectively, showing monocell steps, islands and voids on the (001) surface. c) and d) Tunneling spectra (at 4.2 K) taken on different locations as denoted in image b. Curve 1, measured far from the step, has a V-shaped gap, manifesting c-axis tunneling. Curves 2 and 3, measured near the steps, exhibit ZBCPs of different magnitudes inside U- and V-shaped gaps, respectively. e) Two highly asymmetric tunneling spectra showing pronounced ZBCPs, taken at a different step on the same sample. To demonstrate the spatial variation of the spectra within this scan range we plot in the insets of c) and d) additional data acquired at analogous positions as those presented in the main frames.

the relatively good fit that takes into account such a contribution. The spectra obtained in position 3 show a clear ZBCP inside a gap (fig. 1e). The ZBCP is attributed to ABS formed at the exposed (110) facet. Typically, however, the tunneling spectra acquired on larger (110) crystalline edges exhibited more pronounced ZBCP structures, as depicted in fig. 1f. The fit to the curve in fig. 1e was obtained by taking contributions of (100), (110) and (001) faces, consistent with the corner position (3 in frame a), while that in fig. 1f has only a (110) component.

The main topographic features observed on films that were deposited using a higher laser power were islands and voids of unit-cell height on the (001) surface, as shown in image 2a. Image 2b focuses on a corner between two steps, each of a single unit-cell height, around which the spectra presented in figs. 2c-2d were measured. Generally, tunneling spectra taken far enough (a few nm) from a step or a surface defect (such as holes of sub–unit-cell depth appearing in the image as black dots) exhibited a V-shaped structure, such as curve 1 in fig. 2c. In the vicinity of steps and "point defects", ZBCPs of different magnitudes embedded in relatively symmetric gap structures were observed. This is exhibited by curve 2 (fig. 2c), taken near a (100) monostep facet and showing a U-shaped gap, and by curve 3 (fig. 2d), acquired on a (110) monostep facet, portraying a ZBCP within a V-shaped gap. The difference in the apparent gap between curves 1 and 2 may be due either to local variations in the

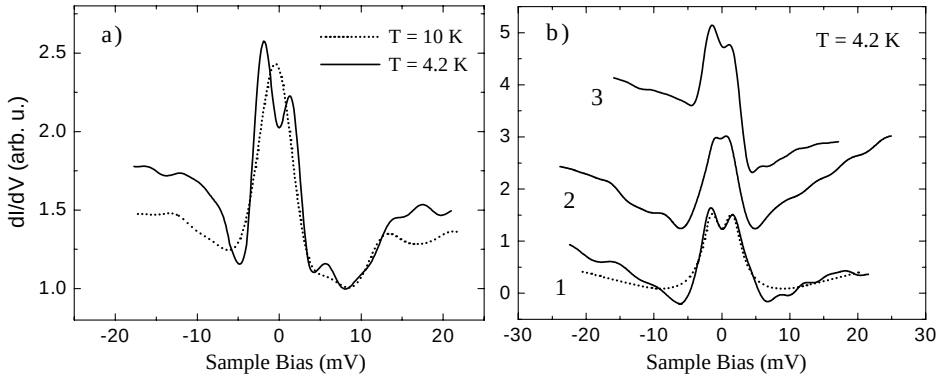

Fig. 3 – Splitting of the ZBCP. a) Two tunneling spectra measured at the same position, one at 4.2 K (solid line) and the other at 10 K (dotted). The clear split seen at 4.2 K is completely washed out at 10 K, signifying a transition into a broken time-reversal symmetry state. b) Three tunneling spectra showing the largest splitting we have detected (3.2 meV peak to peak) (1), the smallest splitting (1.6 meV) (2) and a pronounced asymmetric curve (3). The dotted line is a fit assuming a state of broken time-reversal symmetry having a $d_{x^2-y^2} + is$ order parameter, with $\Delta_d = 30$ meV and $\Delta_s = 0.04\Delta_d$.

oxygen content or to a lifetime broadening effect. Such variations were observed also in STM measurements on single crystals [3]. To demonstrate the typical variance of the spectra within the area shown in image 2b we plot in the insets of 2c) and d) additional characteristics acquired at analogous positions to those presented in the main frames. It is evident that the overall shapes are reproducible along a specific topographic feature. To the best of our knowledge, this is the first time that a clear correlation between tunneling spectra and unit-cell step structure and orientation is demonstrated. This indicates that even a single step of one unit-cell height can alter considerably the *measured* local quasi-particle excitation, pointing out to the apparent discrepancy between theory and experiment, discussed above.

We have also observed tunneling spectra that deviate from the standard d-wave behavior. For example, highly asymmetric ZBCP structures were found on the same sample in similarly looking areas (fig. 2e). Such spectra were predicted to result from scattering by atomic-scale impurities [24, 25]. Unfortunately, we cannot yet specify any typical defect structure, or any special topographic feature, which can be directly related to the appearance of these highly asymmetric tunneling spectra.

We now turn to the issue of splitting of the ZBCP, a manifestation of a state with broken time-reversal symmetry, which we have observed only in overdoped and optimally doped films. In fig. 3a we present two tunneling spectra obtained at the same position on a nominally overdoped film, one taken at 4.2 K, exhibiting a clear splitting of the ZBCP ($\sim$ 2.6 meV peak to peak), and the other at 10 K, where the split is completely washed out. (The lateral position of spectra acquisition was determined at each temperature via the topographic images, although slightly different tip-sample separations may have yielded a small difference in the background.) This temperature dependence indicates that the splitting is due to a broken time-reversal symmetry phase. The peak-to-peak separation we have found in all of our measurements ranged from 1.6 meV (curve 2 in fig. 3b) to 3.2 meV (curve 1). The theoretical fit to curve 1 was obtained using a $d_{x^2-y^2} + is$ order parameter [12], where the magnitude of the subdominant s component, Δ_s, is 4% of the dominant one, Δ_d. We note that we cannot

clearly distinguish between the *is* [12] and the id_{xy} [13] scenarios for the subdominant order parameter, although recent experiments seem to support the latter case [15, 26].

Interestingly, the splitting into two well-resolved peaks we typically observed at 4.2 K was, in many cases, more pronounced than the splitting into two weakly resolved peaks measured in macroscopic planer junction at zero field [4, 5]. The reason for this is that in the macroscopic tunneling junctions the $\mathrm{d}I/\mathrm{d}V$-V curves display an average over large areas, whereas the STM allows probing of specific locations where the splitting is more pronounced. Local probing enables also the observation of highly asymmetric spectra that exhibit a state of broken time-reversal symmetry, such as curve 3.

The fact that splitting was not observed in underdoped samples indicates that spontaneous time-reversal symmetry breaking may take place only beyond some critical doping level, as pointed out by Deutscher [15]. This may be the reason for the contradictory reports of various groups regarding the observation of splitting in zero magnetic field, discussed above. The spatial variations in magnitude of the splitting seen in our nominally overdoped and optimally doped samples may thus be due to fluctuations in the *local* hole doping. The wide superconducting transition exhibited by our samples after completing the STM measurements, as compared to the freshly prepared films, indeed indicates that the samples became non-homogeneous electronically, probably due to inhomogeneous oxygen distribution. Clear evidence for spatial fluctuation in the hole doping was previously observed by STM in other high-T_c superconducting systems [16, 17].

In summary, tunneling spectroscopy measurements on ultrathin epitaxial YBCO films reveal a rich variety of d-wave spectral structures that show pronounced spatial variations with nearly one-to-one correspondence to the surface morphology. Even a single unit-cell step is found to significantly affect the local spectra. The doping and position dependence of the ZBCP splitting suggest that doping plays a major role in the transition to a state with broken time-reversal symmetry, which can occur only beyond some doping level close to optimal doping.

* * *

We are grateful to G. Deutscher for useful discussions. This research was supported in part by the Israel Science Foundation, the Heinrich Hertz Minerva center for high-temperature superconductivity and the Technion fund for the promotion of research.

REFERENCES

[1] Van Harlingen D. J., *Rev. Mod. Phys.*, **67** (1995) 515.
[2] Orenstein J. and Millis A. J., *Science*, **288** (2000) 468.
[3] Wei J. Y. T., Yeh N. C.,Garrigus D. F. and Starsik M., *Phys. Rev. Lett.*, **81** (1998) 2542.
[4] Covinton M., Aprili M., Paraonu E., Green L. H., Xu F., Zhu J. and Mirkinet C.A., *Phys. Rev. Lett.*, **79** (1997) 277.
[5] Krupke R. and Deutscher G., *Phys. Rev. Lett.*, **83** (1999) 4634.
[6] Iguchi I., Wang W., Yamazaki M., Tanaka Y. and Kashiwaya S., *Phys. Rev. B*, **62** (2000) R6131.
[7] Nesher O. and Koren G., *Phys. Rev. B*, **60** (1999) 14893.
[8] Alff L., Beck A., Gross R., Marx A., Kleefisch S., Bauch Th., Sato H., Naito M. and Koren G., *Phys. Rev. B*, **58** (1998) 11197.
[9] Wolf E. L., *Principles of Electron Tunneling Spectroscopy* (Oxford University Press, New York) 1985.

[10] Kashiwaya S., Tanaka Y., Koyanagi M. and Kajimura K., *Phys. Rev. B*, **53** (1996) 2667.
[11] Tanaka Y. and Kashiwaya S., *Phys. Rev. Lett.*, **74** (1995) 3451.
[12] Fogelstrom M., Rainer D., and Sauls J. A., *Phys. Rev. Lett.*, **79** (1997) 281.
[13] Laughlin R. B., *Phys. Rev. Lett.*, **80** (1998) 5188.
[14] Wei J. Y. T., Tsui C. C., van Bentum P. J. M., Xiong Q., Chu C. W. and Wu M. K., *Phys. Rev. B*, **57** (1998) 3650.
[15] Deutscher G., Dagan Y., Kohen A. and Krupke R., *Physica C*, **341-348** (2000) 1629.
[16] Levi Y., Felner I., Asaf U. and Millo O., *Phys. Rev. B*, **60** (1999) R15059.
[17] Levi Y., Millo O., Sharoni A., Tsabba Y., Leitus G. and Reich S., *Europhys. Lett.*, **51** (2000) 564.
[18] de Lozanne A. L., *Supercond. Sci. Technol.*, **12** (1999) R43.
[19] Edwards H. L., Markert J. T. and de Lozanne A. L., *Phys. Rev. Lett.*, **69** (1992) 2967.
[20] Hudson E. W., Pan S. H., Lang K. M., Gupta A. K., Ng K. W. and Davis J. C., *Physica B*, **284-288** (2000) 969.
[21] Yazdani A., Howald C. M., Lutz C. P., Kapitulnik A. and Eigler D., *Phys. Rev. Lett.*, **83** (1999) 176.
[22] Alff L.,Takashima H., Kashiwaya S., Terada N., Ihara H., Tanaka Y., Koyanagi and Kajimura M. K., *Phys. Rev. B*, **55** (1997) R14757.
[23] Salkola M. I., Balatsky A. V. and Scalapino D. J., *Phys. Rev. Lett.*, **77** (1996) 1841.
[24] Tanuma Y., Tanaka Y., Yamashiro M. and Kashiwaya S., *Phys. Rev. B*, **57** (1998) 7997.
[25] Zhu J.-X., Lee T. K., Ting C. S. and Hu C. R., *Phys. Rev. B*, **61** (2000) 8667.
[26] Carmi R., Polturak E., Koren G. and Auerbach A., *Nature*, **404** (2000) 853.